Research Square

Preprints are preliminary reports that have not undergone peer review.
They should not be considered conclusive, used to inform clinical practice,
or referenced by the media as validated information.

Green and Selective Recovery of Lithium from Spent Lithium Iron Phosphate Cathodes via Fenton Reaction

yan zeng

zengyaner@126.com

Xinxiang University

Chaojun Du

Nanyang Institute of Technology

Heng Chen

Xinxiang University

Di Che

Xinxiang University

Jiao Guo

Xinxiang University

Jiangju Si

Xinxiang University

Hui Wang

Xinxiang University

Research Article

Keywords: Photo-fenton, spent $LiFePO_4$ cathodes, selective recovery of lithium, circulating leaching, regenerated $LiFePO_4$

Posted Date: June 23rd, 2026

DOI: https://doi.org/10.21203/rs.3.rs-9627207/v1

License: This work is licensed under a Creative Commons Attribution 4.0 International License.
Read Full License

Additional Declarations: No competing interests reported.

Abstract

Recycling of spent lithium iron phosphate (LFP) batteries is essential for resource sustainability and environmental protection. However, conventional recycling methods often involve harsh conditions, sacrificial reagents, high energy consumption, and secondary pollution. This study proposes a novel and efficient lithium extraction method based on a photo-fenton process to selectively recover lithium from spent $LiFePO_4$ cathodes. Under optimized conditions (800 mmol/L H_2O_2, 100 mmol/L $FeSO_4$, 30°C, 50 g/L solid density, and 30 min reaction time), a lithium leaching efficiency exceeding 99% was achieved with high selectivity. During this process, iron and phosphorus were simultaneously recovered as $FePO_4$ precipitate, while lithium was subsequently separated as high-purity Li_2CO_3. Mechanistic investigations, supported by XRD, XPS, and SEM-EDS analyses, revealed that hydroxyl radicals (•OH), generated from the Fe^{2+}/H_2O_2 Fenton system, attack the olivine structure of $LiFePO_4$. This oxidizes Fe(II) to Fe(III), forming insoluble $FePO_4$ and releasing Li^+ into solution. Notably, ultraviolet irradiation facilitates the regeneration of Fe^{2+} from the reaction products, enabling its reuse and significantly reducing reagent consumption and iron sludge generation. The proposed photo-Fenton method offers an efficient, low-energy, and environmentally benign route for lithium recovery from spent LFP batteries.

1. Introduction

Global climate change has garnered widespread international concern [1]. In response, many countries, including China have committed to achieving "carbon neutrality" or net-zero carbon dioxide emissions by 2050 or 2060 [2, 3]. A cornerstone of this transformation is the replacement of conventional fuel vehicles with electric vehicles (EVs) [4–7].The surge in the EV sector is a major driving force behind the escalating demand and production of lithium-ion batteries (LIBs) for power applications [8–11]. Consequently, the global LIB industry is anticipated to expand to 4.7 TWh by 2030 [12]. Nevertheless, with an average operational lifespan of merely 3–6 years, the proliferation of EVs inevitably results in a massive influx of end-of-life batteries. Recycling valuable materials from spent power LIBs is therefore of strategic importance for reducing production costs, alleviating resource consumption, and minimizing environmental impact [13–15].

A recent report by the European Commission estimated that by 2050, up to 77% of the European Union's lithium demand could be met through secondary sources, primarily from used LIBs [16]. The recycling process for spent LIBs generally involves discharging, dismantling to obtain cathode black mass, followed by leaching and separation operations to recover metal ions [17]. Among various cathode chemistries, lithium iron phosphate (LFP) batteries dominate the EV market due to their safety, long cycle life, and low cost [18–20]

Existing technologies for extracting value-added components from end-of-life LFP cathodes can be categorized into three primary routes: pyrometallurgy, hydrometallurgy, and direct recycling [21–24]. Pyrometallurgy, while simple, suffers from long processing routes, low yield, high energy consumption, and the risk of fluoride volatilization. Direct recycling is relatively green but is limited by challenges such

as high impurity content and inconsistent electrochemical performance of the regenerated materials [25]. Hydrometallurgy remains the predominant approach, typically employing inorganic acids (e.g., H_2SO_4, HCl) [26, 27] or organic acids (e.g., formic, citric, oxalic acid) [28–31] to dissolve the LFP structure. These processes often require oxidants to facilitate redox reactions for metal recovery.

Although inorganic acids enable high lithium leaching efficiencies, they are hindered by limited selectivity, corrosive effects on equipment, and the generation of secondary waste streams. In contrast, organic acids, while milder, often entail higher costs and environmental burdens [32–35].

To improve Li^+ selectivity and address these issues, various oxidizing agents, such as ozone [36], sodium persulfate [37], sodium hypochlorite [38], and hydrogen peroxide [39] have been investigated. These agents oxidize Fe(II) in LFP, converting it into insoluble iron phosphate or hydroxide, thereby liberating the lithium for subsequent recovery. However, these methods often require high reagent concentrations and involve highly corrosive media.

Recently, an in-situ advanced oxidation metallurgy technology based on Fenton oxidation was proposed for selective lithium extraction from $LiFePO_4$ [40]. In this process, Fe(II) is rapidly oxidized to Fe(III), though it generates significant iron sludge. The sludge can be dissolved and reused by adjusting the pH to 2.1 with sulfuric acid, which reduces $FeSO_4$ consumption and cost but still introduces environmental concerns due to the use of mineral acids.

In this study, ultraviolet (UV) irradiation is used to initiate an in-situ photo-Fenton reaction, leveraging its oxidative capability for efficient and selective Li^+ extraction from spent $LiFePO_4$ cathode materials. UV light facilitates the photoreduction of Fe(III) to Fe(II), thereby enabling cyclic regeneration of the Fenton catalyst. This approach significantly reduces iron sludge formation and minimizes the need for sulfuric acid, producing a leachate with negligible iron content and allowing the recovery of high-purity Li_2CO_3. The reaction mechanism was investigated using SEM, XRD, and XPS, supported by thermodynamic and kinetic analyses. We propose that hydroxyl radicals oxidize Fe(II) in $LiFePO_4$ to Fe(III), leading to $FePO_4$ precipitation and Li^+ release into solution, while preserving the original olivine structure.

2. Experiment

2.1 Selective Extraction of Lithium from $LiFePO_4$ Cathode Material

The experimental setup comprised a light source and a reaction vessel (detailed in Text S1). Typically, a predetermined amount of LFP powder, deionized water, and $FeSO_4 \cdot 7H_2O$ were added to the reaction flask. The mixture was stirred and heated to the target temperature. A corresponding volume of H_2O_2 solution was then added dropwise via a pressure-equalizing dropping funnel. After the specified reaction time, the slurry was immediately filtered to separate the leachate and residue for subsequent analysis. Using a one-variable-at-a-time approach, the effects of $FeSO_4$ dosage, slurry density, H_2O_2 concentration,

reaction time and temperature on metal ion leaching efficiency were systematically investigated to determine the optimal conditions.

Post-dilution with deionized water, the leachate was analyzed by ICP-OES (PerkinElmer Optima 8300) to determine Li and Fe concentrations. The separated solid residue, after subsequent rinsing with deionized water, was dried at 80°C for 24 h for further characterization.

The leaching efficiency (η_i) for each element was calculated using Eq. (1):

$\eta_i = c_i V/mw_i \cdot 100$ (1)

where:

c_i (g/L): concentration of element i (Li, Fe) in the leachate;

V (L): volume of the leachate;

m (g): mass of the initial LFP powder;

w_i: mass fraction of element i in the initial powder.

2.2 Recovery of lithium

To recover lithium from the leach solution, the pH of the Li-rich leachate was first elevated to 12 using NaOH, followed by centrifugation to eliminate residual iron impurities. Next, sodium carbonate was added to the purified solution, and the precipitation process was conducted at 95°C for 1 h. The resulting Li_2CO_3 precipitate was subsequently collected by filtration, rinsed with boiling deionized water, and finally dried to achieve a high-purity product.

3. Results and discussion

3.1 Effects of different leaching parameters

A systematic study was conducted to evaluate the influence of critical operational parameters on the efficiency and selectivity of lithium leaching from $LiFePO_4$ in the photo-Fenton system. The parameters investigated included reagent concentrations, slurry density, temperature, and reaction time.

The effects of H_2O_2 and $FeSO_4$ concentrations were first examined at 30°C, 50 g/L solid density, and a 30-minute reaction time. As shown in Figs. 1(a) and 1(b), both reagents are essential for effective leaching. In the absence of H_2O_2 or $FeSO_4$, lithium leaching efficiencies were only 0.3% and 6.4%, respectively.

With an increase in H_2O_2 concentration from 0 to 800 mmol/L, the lithium leaching efficiency experienced a dramatic rise, reaching 99.3%. However, a further increase to 1200 mmol/L resulted in

only a marginal increase of 0.04%. Similarly, increasing $FeSO_4$ concentration from 0 to 100 mmol/L boosted Li recovery to 99.3%, with negligible enhancement beyond this point. The dramatic increase in leaching efficiency is attributed to the accelerated generation of •OH radicals via the Fenton reaction between Fe^{2+} and H_2O_2, which promotes the oxidation of Fe(II) to Fe(III) in LFP and the consequent release of Li^+. The 6.4% leaching efficiency observed without added $FeSO_4$ suggests that H_2O_2 can also react directly with Fe(II) in LFP via a heterogeneous Fenton-like reaction to produce •OH on the particle surface [37].

Notably, H_2O_2 was added dropwise to prevent rapid gas generation and solution foaming, which could cause overflow. The exothermic nature of the reaction also necessitated controlled addition to manage heat generation.

The influence of slurry density (40–70 g/L) is shown in Fig. 1(c). As density increased from 50 to 70 g/L, Lithium leaching efficiency decreased from 99.3% to 48.1%. Lower slurry densities provide greater contact area between the LFP particles and •OH radicals in solution, thereby improving leaching efficiency [38]. Consequently, 50 g/L was selected as the optimal slurry density.

The effects of reaction time (5–30 min) and temperature (30–90°C) are presented in Fig. 1(d). At all temperatures, Lithium leaching efficiency increased with time but decreased with increasing temperature. At 30°C, efficiency rose from 72.0% (5 min) to 99.3% (30 min), demonstrating superior performance under mild conditions. The high efficiency (72%) achieved within just 5 minutes confirms the rapid kinetics of the Fenton-driven leaching process, consistent with previous reports [37]. Thus, 30°C and 30 minutes were chosen as the optimal temperature and time.

In summary, under the optimized conditions of 800 mmol/L H_2O_2, 100 mmol/L $FeSO_4$, 50 g/L slurry density, 30°C, and 30 minutes, a Lithium leaching efficiency of 99.3% was achieved.

3.2 Kinetic analysis

The leaching behavior was further analyzed using the shrinking core model to elucidate the underlying reaction mechanism, a methodology widely adopted for characterizing heterogeneous systems [39]. The model considers three potential rate-limiting steps, described by the following equations:

Gas film diffusion control model: $\mathrm{X}=\mathrm{k}_1\mathrm{t}$ (2)

Surface chemical reaction control model: $1\text{-}\left(1\text{-}\mathrm{X}\right)^{\frac{1}{3}}=\mathrm{k}_2\mathrm{t}$ (3)

Product layer diffusion control model: $1\text{-}3\left(1\text{-}\mathrm{X}\right)^{\frac{2}{3}}+2\left(1\text{-}\mathrm{X}\right)=\mathrm{k}_3\mathrm{t}$ (4)

In these equations, X denotes the leaching efficiency of lithium, and t represents the reaction time in minutes. The parameters k_1, k_2, and k_3 are defined as the apparent rate constants corresponding to the different kinetic steps.

Fitting the experimental data obtained under optimized conditions across different temperatures (30–90°C) and reaction times (5–30 min) revealed that the surface chemical reaction control model provided the best fit, with regression coefficients (R^2) exceeding 0.9877. Detailed fitting parameters are provided in Table S1 and Figure S1.

$$Ea = -RT\ln\left(\frac{k}{A}\right)$$

5

Fitting the experimental data obtained under optimized conditions across different temperatures (30–90°C) and reaction times (5–30 min) revealed that the surface chemical reaction model provided the best fit, with regression coefficients (R^2) exceeding 0.9877. Detailed fitting parameters are provided in Table S1 and Figure S1.

The apparent activation energy (Ea) was estimated from the Arrhenius Eq. (5) to be 21.89 kJ·mol^{-1} (Fig. 2). The negative correlation between rate constant and temperature suggests a decreasing reaction rate with increasing temperature, consistent with experimental observations [40]. The kinetic analysis reveals that the leaching process is governed by a surface chemical reaction as the rate-determining step. This finding, combined with the observed decline in leaching efficiency at elevated temperatures, can be attributed to the thermal degradation of H_2O_2, which reduces the availability of reactive oxygen species necessary for the oxidative extraction of lithium.

3.3 Mechanism of lithium leaching

The reaction mechanism was further investigated by characterizing the leaching residues using XRD, XPS, and SEM. As the leaching process progressed from 0 to 30 min, the XRD patterns (Figure S2) revealed a clear phase transition from $LiFePO_4$ to $FePO_4$ (PDF# 34–0134), as evidenced by the diminishing intensity of $LiFePO_4$ peaks and the corresponding rise of $FePO_4$ peaks. Importantly, no other crystalline phases were observed, suggesting a direct topotactic transformation. This finding was consistent with the XPS and SEM results, which showed a progressive oxidation of surface iron and an evolution in particle morphology.

To investigate the chemical states of elements in the residue, XPS analysis was conducted on the solid sample. The Li 1s peak was observed to almost completely disappear. More importantly, We observed a distinct shift of the Fe $2p_3/_2$ and Fe $2p_1/_2$ peaks to higher binding energies, which is indicative of Fe(III) formation and consequently substantiates the oxidation of iron from + 2 to + 3 during leaching [38, 41] (Fig. 3(b)). These results confirm that the primary constituent of the leaching residue is $FePO_4$.

SEM images (Fig. 4) showed that the residual $FePO_4$ retained an olivine-like morphology similar to the original LFP, without structural collapse. This preservation of microstructure is beneficial for the solid-state transformation and the subsequent release of Li^+ into solution.

Compared to traditional oxidants such as $S_2O_8^{2-}$ [42] (2.01 V) and H_2O_2 [43](1.776 V), the hydroxyl radical (•OH) generated in the Fenton system possesses a higher standard redox potential (~ 2.8 V) [37], enabling rapid oxidation of Fe(II) in LFP to Fe(III). According to the classical Fenton mechanism, Fe^{2+} activates H_2O_2 to generate •OH, which then oxidizes $LiFePO_4$ to Li^+ and $FePO_4$[37]. This pathway allows for the selective and efficient recovery of aqueous Li^+ and solid $FePO_4$ from spent LFP, in agreement with our experimental results.

3.4 Visible light effects and circulating leaching

The conventional Fenton reaction rapidly consumes Fe(II), leading to Fe(III) accumulation and iron sludge formation [44]. According to photo-Fenton principles, ultraviolet (UV) light can promote the reduction of Fe^{3+} to Fe^{2+} and enhance •OH generation. In this study, UV irradiation was introduced to facilitate the dissolution and reduction of iron species, enabling Fe^{2+} regeneration (Figure S3). As illustrated, Fe^{2+} is oxidized to Fe^{3+} after the Fenton reaction but can be photoreduced back to active Fe^{2+} under UV light for use in subsequent cycles.

Cyclic leaching tests (Figure S4) showed that lithium leaching efficiency remained above 90% for the first three cycles, declining to 41% by the sixth cycle. Concurrently, the lithium concentration in solution accumulated to approximately 1.1 g/L, indicating sustained •OH generation and selective lithium leaching even without fresh Fe(II) addition.

during the reaction

Figure 5 shows a schematic representation of the proposed mechanism underlying the photo-Fenton process. The process is initiated by the generation of highly oxidative hydroxyl radicals (•OH) through dual pathways: (i) the homogeneous Fenton reaction (Fe^{2+}/H_2O_2) and (ii) a heterogeneous Fenton-like reaction involving H_2O_2 and surface Fe(II) species on the LFP particles. These •OH radicals subsequently attack the LFP structure, oxidizing Fe(II) to Fe(III) and leading to the formation of insoluble $FePO_4$, which retains the olivine framework, while Li^+ ions are concomitantly released into the solution. A key feature of this system is the role of UV light, which promotes the photo-reduction of Fe(III) back to Fe(II), thereby enabling effective catalyst regeneration and reducing the consumption of $FeSO_4$ by over 70%. Nevertheless, prolonged operation over multiple cycles results in the gradual accumulation of insoluble Fe(III) species, which ultimately contributes to a decline in process efficiency.

3.5 Characterization of Regenerated $LiFePO_4$ Cathode Materials

XRD patterns of the recovered $FePO_4$ and Li_2CO_3 (Figures S2 and S5) matched well with their standard reference patterns, indicating high phase purity. The recovered $FePO_4$ and Li_2CO_3 was used to resynthesize $LiFePO_4$ via a solid-state roasting method at 750°C [37]. The regenerated LFP exhibited an orthorhombic olivine structure with a honeycomb-like morphology, as confirmed by SEM and XRD (Figure S6).

The regenerated LFP cathode was assembled into coin cells for electrochemical evaluation at 25°C. Cyclic voltammetry (Figure S8(a)) showed characteristic redox peaks at approximately 3.26 V (Fe^{3+}/Fe^{2+} reduction) and 3.57 V (Fe^{2+}/Fe^{3+} oxidation), corresponding to Li^+ insertion and extraction, respectively [45].

The regenerated $LiFePO_4$ cathode not only delivered a superior initial discharge capacity of 156.87 mAh/g at 0.2C with an average coulombic efficiency of 98.52% (Figure S8(b)), but also exhibited outstanding cycling stability. Remarkably, it retained 88.10% of its initial capacity after 200 cycles at 0.5C (Figure S8(c)), underscoring its potential for longterm application.

4. Conclution

In this study, a novel selective lithium leaching system based on a photo-Fenton process was successfully developed. Under optimal conditions (30°C, 30 min, 800 mmol/L H_2O_2, 100 mmol/L $FeSO_4$, 50 g/L slurry density), the system achieved a lithium leaching efficiency of 99.3% with complete selectivity. A key advantage of this process is the reusability of the $FePO_4$ residue, which remained effective for up to six cycles, thereby substantially minimizing iron sludge generation. The leaching residue and the lithium-containing solution were processed to yield relatively pure $FePO_4$ and Li_2CO_3, respectively, as confirmed by XRD, SEM, and XPS analyses. These intermediates were then successfully employed as precursors to resynthesize $LiFePO_4$ via a solid-state roasting method. The regenerated $LiFePO_4$ cathode material exhibited excellent electrochemical performance, delivering an initial discharge capacity of 156.87 mAh/g at 0.2C and retaining 88.1% of its capacity after 200 cycles at 0.5C. Overall, this photo-Fenton approach offers an efficient, low-energy, and environmentally benign strategy for the selective recycling of lithium from spent $LiFePO_4$ batteries.

Declarations

Author Contribution

Yan Zeng conceived and designed the study, performed the experiments, analyzed the data, and wrote the manuscriptChaojun Du proposed the concept;Heng Chen analyzed the data, performed the statistical analysis;Di Che performed the experiments;Jiao Guo supervised the study;Jiangju Si developed the methodology;Hui Wang revised the manuscript ;All authors reviewed the manuscript.

References

1. Bank MS, Swarzenski PW, Duarte CM, Rillig MC, Koelmans AA, Metian M, Wright S, Provencher JF, Sanden M, Jordaan A, Wagner M, Thiel M, Ok YS (2021) Global plastic pollution observation system to aid policy. Environmental Science & Technology, 55:7770–7775. https://orcid.org/0000-0001-5194-7171

2. Rogelj J, Geden O, Cowie A, Reisinger A (2021) Net-zero Emissions Targets are Vogue: Three ways to Fix: To limit warming, action plans from countries and companies must be fair, rigorous and transparent. Nature 591:365–368. https://doi.org/10.1038/d41586-021-00662-3
3. Wang F, Harindintwali JD, Yuan Z, Wang M, Wang F, Li S, Yin Z, Huang L, Fu Y, Chang S, Zhang L, Rinklebe J, Yuan Z, Zhu Q, Xiang L, Tsang DCW, Xu L, Jiang X, Liu, Wei N, Kästner M, Zou Y, Ok YS, Shen J, Peng D, Zhang W, Barceló D, Zhou Y, Bai Z, Li B, Zhang B, Wei K, Cao H, Tan Z, Zhao LB, He X, Zheng J, Bolan N, Liu X, Huang C, Dietmann S, Luo M, Sun N, Gong J, Gong Y, Brahushi F, Zhang T, Xiao C, Li X, Chen W, Jiao N, Lehmann J, Zhu YG, Jin H, Schäffer A, Tiedje J, Chen M (2021) Technologies and perspectives for achieving carbon neutrality. Review 2:100180–100202. https://doi.org/10.1016/j.xinn.2021.100180
4. Gulley AL, McCullough EA, Shedd KB (2019) China's domestic and foreign inffluence in the global cobalt supply chain. Resour Policy 62:317–323. ttps://doi.org/10.1016/j.resourpol.2019.03.015
5. Yang Y, Okonkwo EG, Huang G, Xu S, Sun W, He Y (2021) On the sustainability of lithium ion battery industry-a review and perspective. Energy Storage Mater 36:186–212. https://doi.org/10.1016/j.ensm.2020.12.019
6. Diouf B (2024) The electric vehicle transition,.Environmental Science: Advances, 2024, 3: 332–345.https://doi.org/10.1039/D3VA00322A
7. Zuo w, Li Y, Wang Y (2019) Research on the optimization of new energy vehicle industry research and development subsidy about generic technology based on the three-way decisions. J Clean Prod 212:46–55. https://doi.org/10.1016/j.jclepro.2018.11.263
8. Li R, Li K, Wang W, Zhang F, Tian S, Ren Z, Zhou Z (2023) Highly selective and green recovery of lithium ions from lithium iron phosphate powders with ozone. Front Chem Sci Eng 17:749–758. https://doi.org/10.1007/s11705-022-2261-0
9. Li YJ, Dong YP, Shi P, Ren ZQ, Zhou ZY (2024) Selective recovery of lithium from lithium iron phosphate. J Power Sources 598:234158–234165. https://doi.org/10.1016/j.jpowsour.2024.234158
10. Ding YJ, Fu JY, Zhang SG, He XF, Zhao BH, Ren J, Zhong JH, Liu ZJ (2024) Advances in recycling $LiFePO_4$ from spent lithium batteries: a critical review. Sep Purif Technol 338:126551–126562. https://doi.org/10.1016/j.seppur.2024.126551
11. Zhang M, Wang L, Wang S, Ma T, Jia F, Zhan C (2023) A Critical Review on the Recycling Strategy of Lithium Iron. Small Methods 7:2300125–2300138. https://doi.org/10.1002/smtd.202300125
12. Link S, Schneider L, Stephan A, Weymann L, Plötz P (2025) Feasibility of meeting future battery demand via domestic cell production in Europe. Nat Energy 10:526–534. https://doi.org/10.1038/s41560-025-01722-y
13. Lai X, Huang Y, Deng C, Gu H, Han X, Zheng Y, Ouyang M (2021) Sorting, regrouping, and echelon utilization of the large-scale retired lithium batteries: a critical review. Renew Sustainable Energy Reviews 146:111162–111182. https://doi.org/10.1016/j.rser.2021.111162
14. Fujita T, Chen H, Wang KT, He CL, Wang YB, Dodbiba G, Wei YZ (2021) Reduction, reuse and recycle of spent Li-ion batteries for automobiles: a review. Int J Minerals Metall Mater 28:179–192.

https://doi.org/10.1007/s12613-020-2127-8

15. Pradhan S, Nayak R, Mishra S (2022) A review on the recovery of metal values from spent nickel metal hydride and lithium-ion batteries. Int J Environ Sci Technol 19:4537–4554. https://doi.org/10.1007/s13762-021-03356-5
16. Meegoda J, Charbel G, Watts D (2024) Second Life of Used Lithium-Ion Batteries from Electric Vehicles in the USA, Environments, 11:97–124. https://doi.org/10.3390/environments11050097
17. Zhang X, Li L, Fan E, Xue Q, Bian Y, Wu F, Chen R (2018) Toward sustainable and systematic recycling of spent rechargeable batteries. Chem Soc Rev 47:7239–7302. https://doi.org/10.1039/C8CS00297E
18. China Industrial Association of Power Sources (2021) China's top 20 power lithium-ion battery companies in terms of installed capacity in 2020. http://www.ciaps.org.cn/news/show-htm-itemid-37907.html
19. Choudhary N, Yadav S, Gohil H, Tothadi S, Paital AR (2025) A Recyclable Cooperative Approach for Selective Lithium Recovery from Industrial-Grade Spent Lithium-Ion Battery Black Mass via Oxidative Delithiation and Complexation Mechanism. Angew Chem Int Ed 64:202509571–202509582. https://doi.org/10.1002/anie.202509571
20. Ghossein N, Sari A, Venet P (2019) Effects of the hybrid composition of commercial lithium-ion capacitors on their floating aging. IEEE Trans Power Electron 34:2292–2299. https://hal.science/hal-01864487v1
21. Santos C, Alves J, Silva S, Sita L, Silva P, Almeida L, Scarminio J (2018) A closed-loop process to recover Li and Co compounds and to resynthesize $LiCoO_2$ from spent mobile phone batteries. J Hazard Mater 362:458–466. https://doi.org/10.1016/j.jhazmat.2018.09.039
22. Meng Q, Zhang Y, Dong P (2017) A combined process for cobalt recovering and cathode material regeneration from spent $LiCoO_2$ batteries: Process optimization and kinetics aspects. Waste Manag 71:372–380
23. Zhao Y, Yuan Y, Jiang L, Wen J, Wang H, Guan R, Zhang J, Zeng G (2019) Regeneration and reutilization of cathode materials from spent lithium-ion batteries. Chem Eng J 383:123089–123107
24. Liu C, Lin J, Cao H, Zhang Y, Sun Z (2019) Recycling of spent lithium-ion batteries in view of lithium recovery: A critical review. J Clean Prod 228:801–813
25. Wu D, Wang D, Liu Z, Rao S, Zhang K (2022) Selective recovery of lithium from spent lithium iron phosphate batteries using oxidation pressure sulfuric acid leaching system. Trans Nonferrous Met Soc China 32:2071–2079
26. Song Y, Xie B, Song S, Lei S, Sun W, Xu R, Yang Y (2021) Regeneration of $LiFePO_4$ from spent lithium-ion batteries via a facile process featuring acid leaching and hydrothermal synthesis. Green Chem 23:3963–3971
27. Li H, Xing S, Liu Y, Li F, Guo H, Kuang G (2017) Recovery of lithium, iron, and phosphorus from spent $LiFePO_4$ batteries using stoichiometric sulfuric acid leaching system. ACS Sustain Chem Eng

5:8017–8024
28. Chai X, Yu X, Shen Q, Li X, Lin Y, Cai W, Yuan Y (2024) Study on green closed-loop regeneration of waste lithium iron phosphate based on oxalic acid system. Waste Manag 181:168–175
29. Ding Y, Fu J, Zhang S, Zhao B, Ren J, Zhong J, Liu Z (2024) Advances in recycling $LiFePO_4$ from spent lithium batteries: a critical review. Sep Purif Technol 338:126551–126562
30. Mahandra H, Ghahreman A (2021) A sustainable process for selective recovery of lithium as lithium phosphate from spent $LiFePO_4$ batteries. Resour Conserv Recycling 175:105883–105893
31. Wang Y, Wu J, Hu G, Ma W (2024) Recovery of Li and Fe from spent lithium iron phosphate using organic acid leaching system. Trans Nonferrous Met Soc China 34:336–346
32. Yu HX, Yang HT, Chen KC, Yang LM, Huang MT, Wang ZH, Lv H, Xu CX, Chen L, Luo XB (2024) Non–closed–loop recycling strategies for spent lithium–ion batteries: current status and future prospects. Energy Storage Mater 67:103288–103310
33. Yu H, Zhao D, Chen K, Huang M, Yang H, Yang L, Wang Z, Chen L, Ding X, Lv H, Luo X (2025) A novel method to repair and upgrade spent LFP cathode material by inherent Al impurity doping. Resour Conserv Recycl 223:108523–108532
34. Hang R, Lei Y, Wei G, Wang Y, Yu Z, Qu J, Qi T (2023) Recovery of $LiFePO_4$ from spent lithiumion batteries by pyrolysis flotation. J Nonferrous Met 5(33):1585–1600
35. Wu J, Xiao L, Shen L, Ran JJ, Zhong H, Zhu YR, Chen (2024) Recent advancements in hydrometallurgical recycling technologies of spent lithium-ion battery cathode materials. Rare Met 43(3):879–899
36. Li R, Li K, Wang W, Zhang F, Tian S, Ren Z, Zhou Z (2023) Highly selective and green recovery of lithium ions from lithium iron phosphate powders with ozone. Front Chem Sci Eng 17:749–758
37. Wu YZ, Li GM, Zhao SQ, Yin YW, Wang B, He WZ (2024) Selective recovery of lithium from spent lithium iron phosphate batteries. Waste Manag Res 32:2071–2079
38. Kong Y, Yuan L, Liao Y, Shao Y, Hao S, Huang Y (2023) Efficient separation and selective li recycling of spent $LiFePO_4$ cathode. Adv Energy Mater 3:300053–300064
39. Fu DJ, Zhou W, Liu JL, Zeng SZ, Wang LY, Liu WF, Yu X, Liu XG (2024) A facile route for the efficient leaching, recovery, and regeneration of lithium and iron from waste lithium iron phosphate cathode materials. Sep Purif Technol 342:127069–127081
40. Chen X, Yuan L, Yan S, Ma X (2023) Self-activation of Ferro-chemistry based advanced oxidation process towards in-situ recycling of spent $LiFePO_4$ batteries. Chem Eng J 471:144343–144352
41. Choudhary N, Yadav S, Gohil H, Tothadi S, Paital AR (2025) A Recyclable Cooperative Approach for Selective Lithium Recovery from Industrialgrade Spent Lithium-Ion Battery Black Mass via Oxidative Delithiation and Complexation Mechanism. Angew Chem Int Ed 14(363):132044–132055
42. Wang J, Wang S (2018) Activation of persulfate (PS) and peroxymonosulfate (PMS) and application for the degradation of emerging contaminants. Chem Eng J 334:1502–1517

43. Yang S, Wang P, Yang X, Shan L, Zhang W, Shao X, Niu R (2010) Degradation efffciencies of azo dye Acid Orange 7 by the interaction of heat, UV and anions with common oxidants: persulfate, peroxymonosulfate and hydrogen peroxide. J Hazard Mater 179:552–558
44. Bello MM, Abdul A, Raman A, Asghar A (2019) A review on approaches for addressing the limitations of Fenton oxidation for recalcitrant wastewater treatment. Process Saf Environ Prot 126:119–140
45. Zhou J, Yu H, Mei Y, Xu L, Liu L, Hu J, Hou H, Yang J (2026) Green and selective recovery of lithium by phosphate base leaching system from spent lithium iron phosphate batteries. Waste Manag 209:115196–115205

Figures

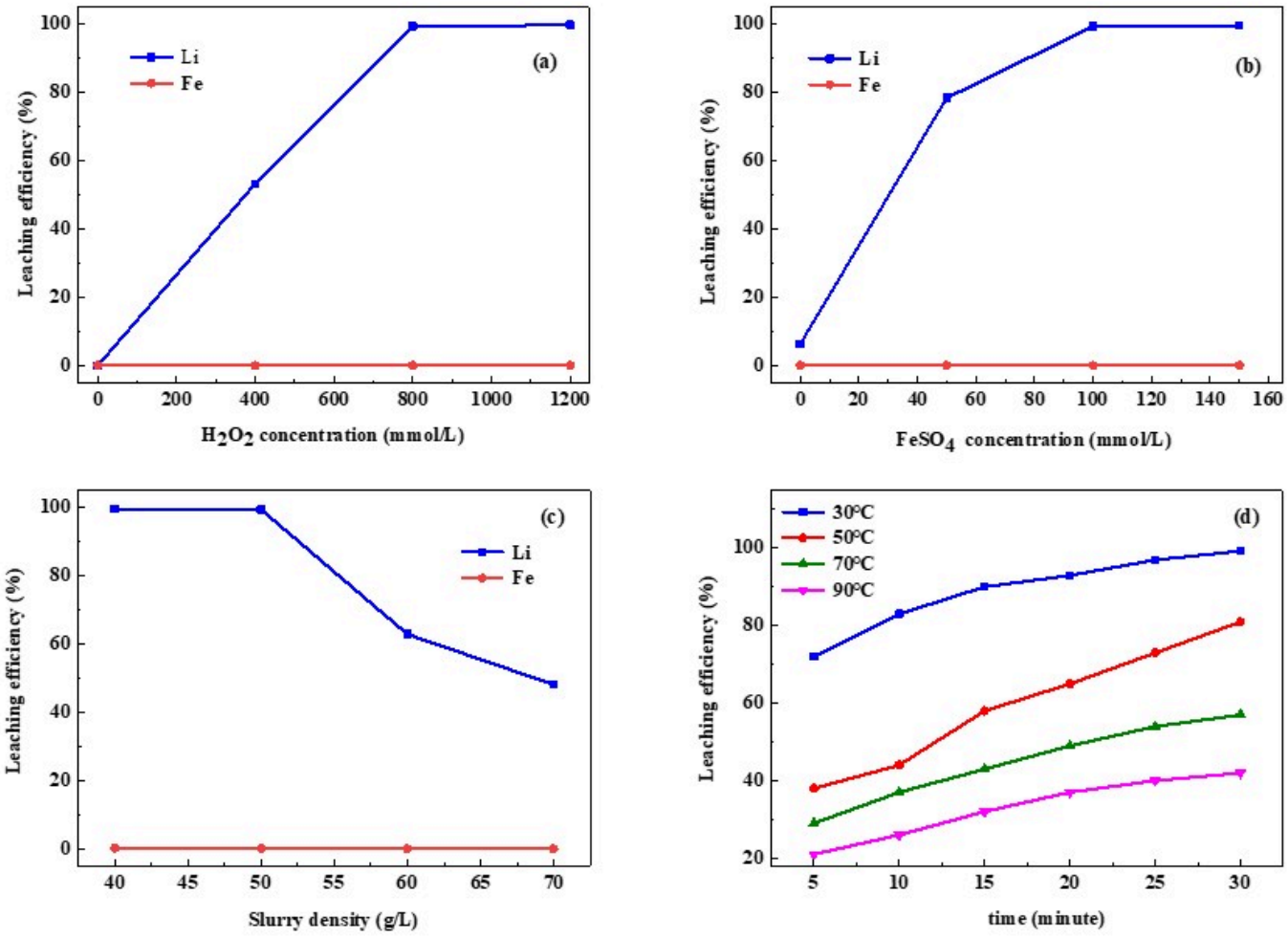


Figure 1

Effect of (a) H_2O_2 concentration, (b) $FeSO_4$ concentration, (c) slurry density, and (d) reaction temperature and time on lithium leaching efficiency. Standard conditions (unless specified): 800 mmol/L H_2O_2, 100

mmol/L $FeSO_4$, 30°C, 30 min, 50 g/L slurry density.

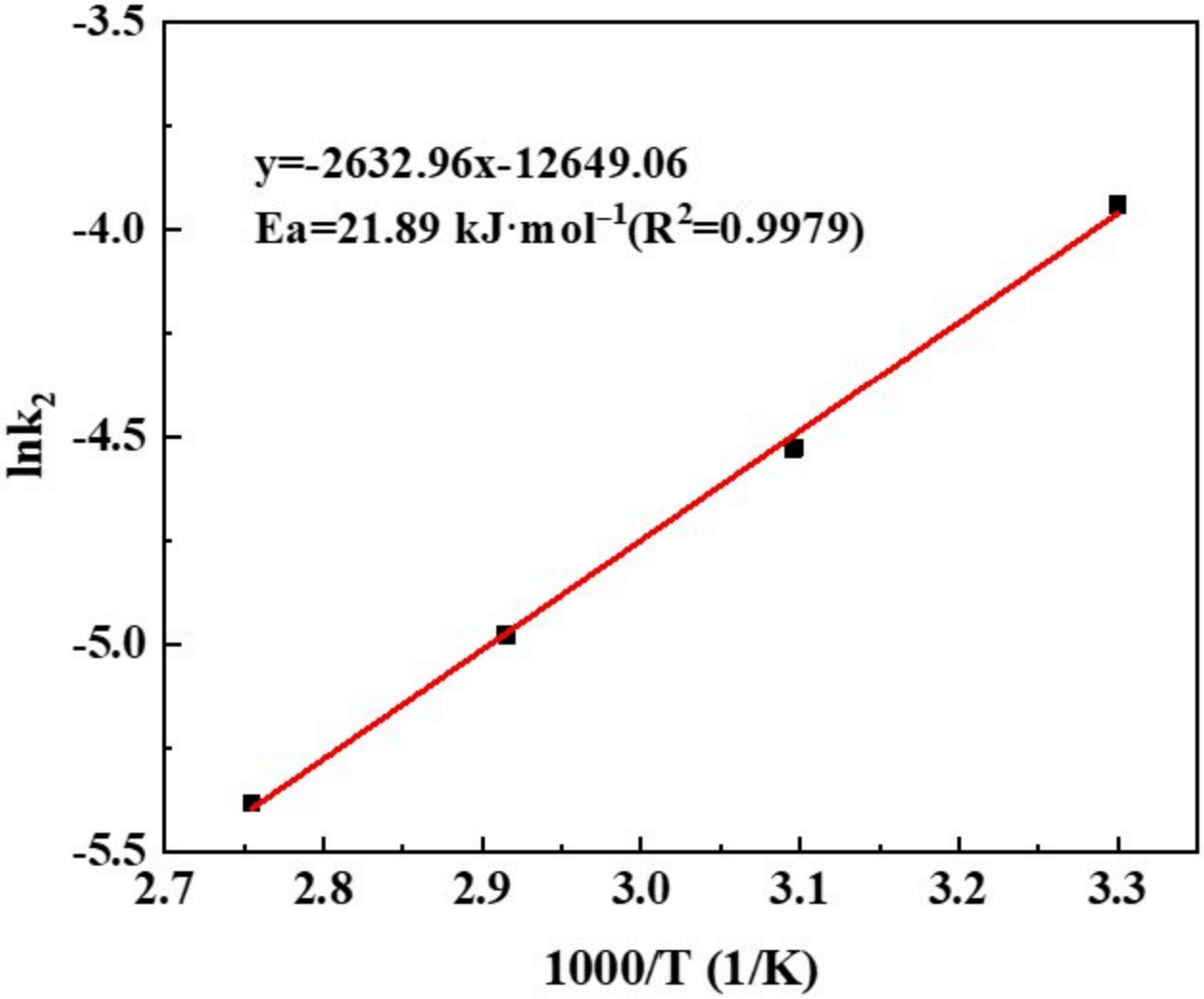


Figure 2

Arrhenius plot of lnk^{-1}/T

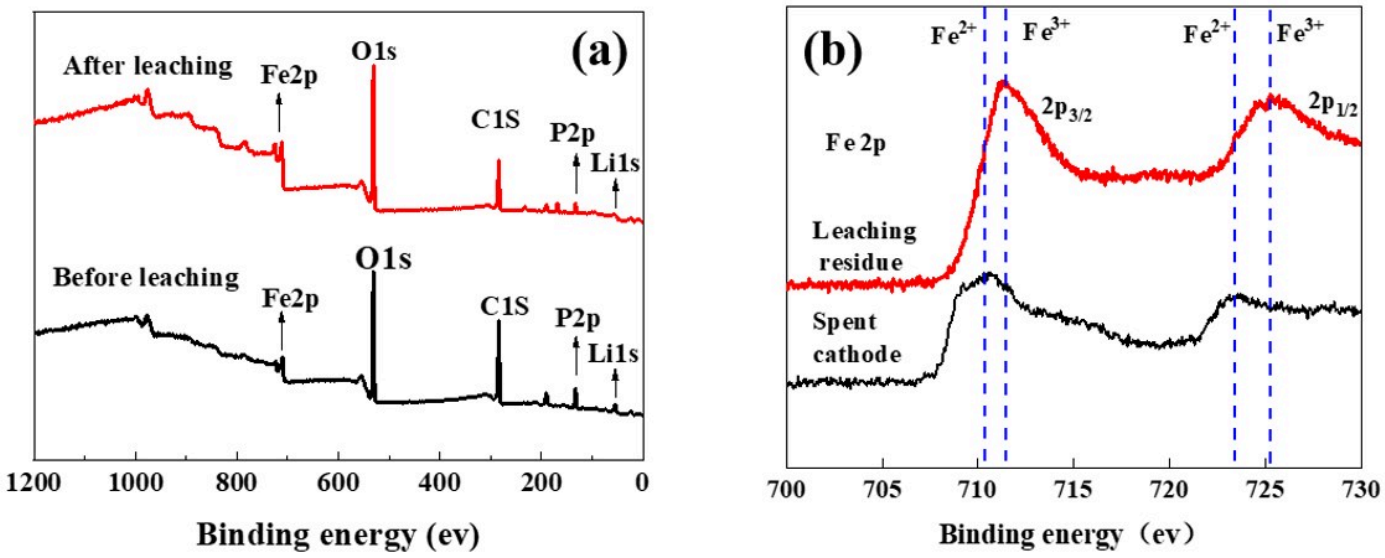


Figure 3

XPS spectra of the spent $LiFePO_4$ cathode powder and leaching residue

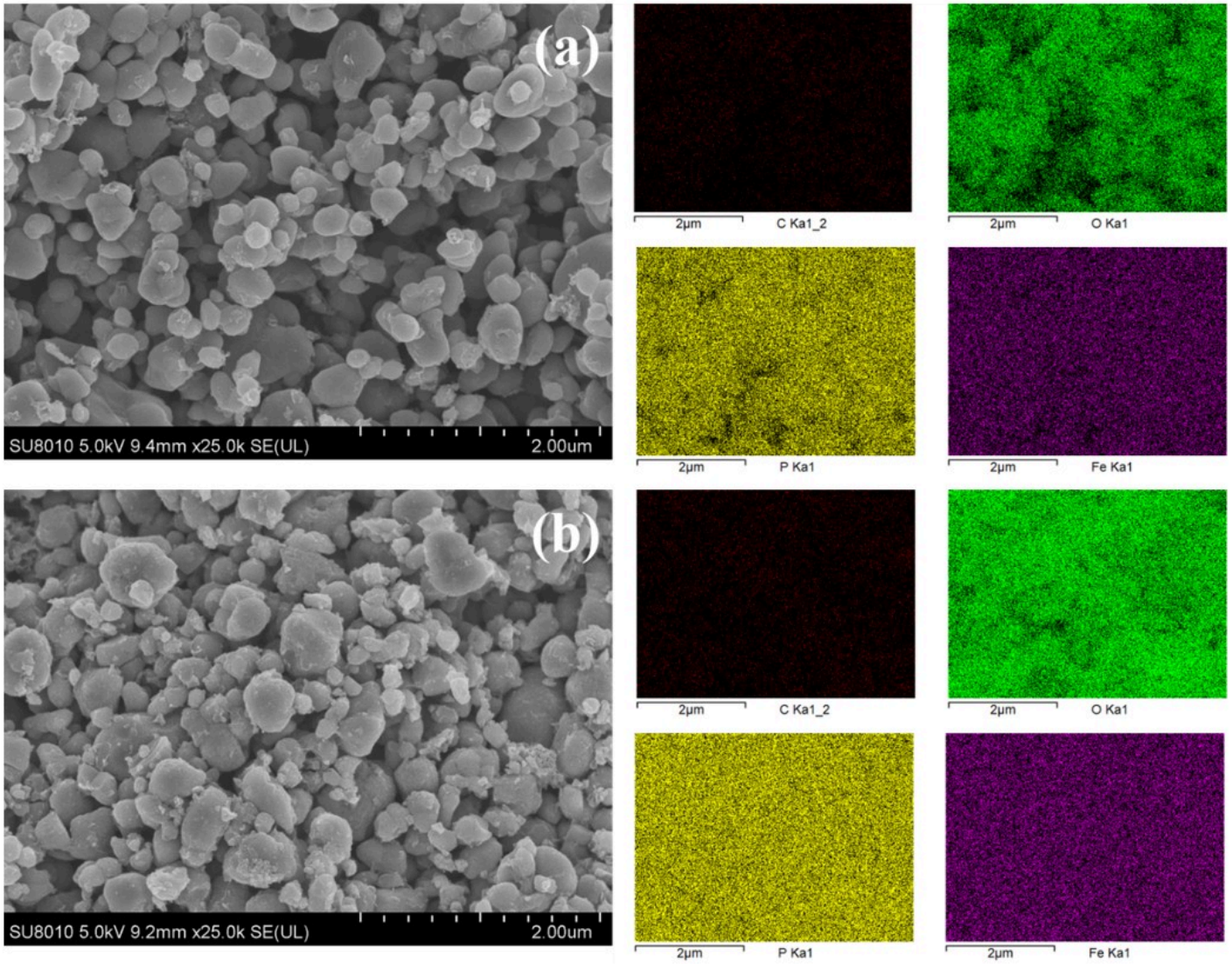


Figure 4

SEM images of (a) the spent $LiFePO_4$ cathode powder and (b) the leaching residue.

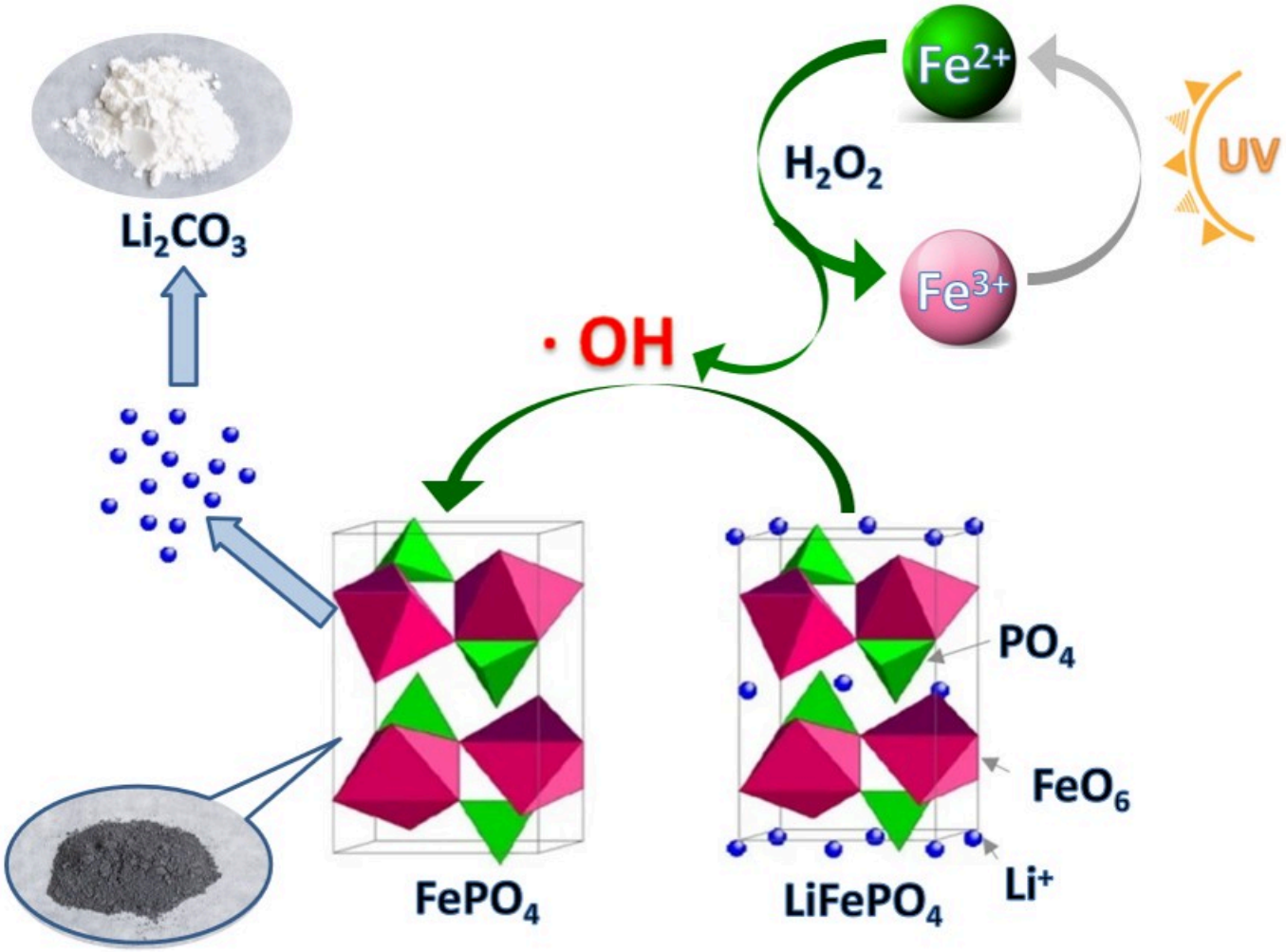


Figure 5

Schematic illustration of the detailed transformation of different products during the reaction

Supplementary Files

This is a list of supplementary files associated with this preprint. Click to download.

- SupportingInformation.docx